International Review of Aerospace Engineering (I.RE.AS.E), Vol. 10, N. 5
ISSN 1973-7459 October 2017

Hyperspectral Remote Sensing Imagery Processing Focused on Forest Applications

Vladimir V. Kozoderov[1], Timofei V. Kondranin[2], Egor V. Dmitriev[2, 3]

Abstract – *Imaging spectrometers with hundreds of spectral channels in visible and infrared regions are designed by various companies to enhance the information content of the relevant hyperspectral imagery processing compared to common-used multispectral systems. We review some sources on this particular subject to show the priorities of the hyperspectral approach before the multispectral one in forest and agriculture applications. There is also a discussion about some results of the information products obtained by an imaging spectrometer produced in Russia for a test area, where the ground-based forest inventory map is available to compare the traditional approaches and the newly defined ones. The related applications concern the pattern recognition of forest classes with different species and age on the test area using the airborne hyperspectral imagery processing.* **Copyright © 2017 Praise Worthy Prize S.r.l. - All rights reserved.**

Keywords*:* *Remote Sensing, Multispectral Images, Hyperspectral Images, Pattern Recognition, Forest Vegetation, Agriculture*

I. Introduction

Forest applications evolved in the pre-satellite era for reconnaissance and similar other purposes using aviation facilities. Visual decoding of air-photo-survey materials was among the main instruments of forest objects recognition by a human eye and an experienced operator in the first analysis results before computer era. Humans are the best pattern recognizers, though we do not yet understand how they do that without any computer means.

The multi-spectral Landsat satellite systems with precision instrumentations have been developed since 1972 [1]-[3]. The relevant satellite images serve to characterize and detect changes in the land cover and land use of the world. The existing methods for land cover change monitoring on medium scale (10–50 m) typically employ Landsat data to capture global land conditions and dynamics.

As multi-spectral imagery of remote sensing appears, computational procedures of the related object pattern recognition have become the main tool of computer applications. In particular, one of the first procedures of this kind concerns classifying agricultural plants [4] using an airborne optical system.

The neighborhood is a mathematical category of understanding a measure of proximity between the object classes in the texture analysis of pattern recognition and scene analysis methods.

The neighborhood in graphs concept was given in [5] to introduce this measure.

The appearance of the first optical systems of airborne and space-borne observations of the Earth and the atmosphere stimulated this discipline.

The land surface objects called patterns gave a basis for their recognition using remotely sensed imagery processing procedures. These studies originated from previous science and technology developments and are called now cognitive technology [6]. The Charge Coupled Device (CCD) technology [7] enables to construct sensors in the newly defined type of remote sensing instruments within a specified “broom” construction that gives spectral values for each pixel of the image.

The hyperspectral technology of imagery processing in multi-dimensional feature space given by hundreds of spectral bands serves to combine advances in spatial resolution and spectroscopy [8]. This technology looks nowadays as the most promising in the retrieval procedures of the object reflectivity taking into account radiometric, atmospheric and other distortions of registered spectral values [9]. Thin nuances of the object pattern recognition get feasible under the related techniques though optimization procedures are needed to diminish the possible redundancy of the spectral bands in the hyperspectral domain due to the possible interdependencies between neighboring channels.

Cognitive technologies are based on attempts to create artificial intelligence systems of data mining [10].

Machine-learning algorithms are used to recognize patterns. The relevant methods include the following stages: creating alphabets of object classes on the images, defining characteristic features of these classes and elaborating computational procedures concerning decision making rules of belonging among the current pixels to the considered object classes [11].

Starting in the 1980s as an attempt to unite scientists in the field of observing land surface – atmosphere

https://doi.org/10.15866/irease.v10i5.12893

interactions on different scales with the ultimate goal of climate change [12], these studies are urgent encompassing an upscale integration of the related models and remote sensing applications.

The first techniques of automated pattern recognition for optical remote sensing images were given in [13], [14]. The first optical image processing applications dealt with the problem of computer vision to understand and simulate the nature of the phenomena that create the image. The emerged problem was how to define an objective function for the optimal solution of the interpretation of visual information. Any image processed is considered in the contextual constraints of its objects [15].

The consideration of the image distortion problem due to the atmosphere as scattering and absorbing media was also among the computational approaches of image processing [16]. This part of studies embedded remote sensing of soils and vegetation [17] and the atmospheric correction of remotely sensed images [18]. In parallel, the initial statements of computer vision were developed, which dealt with a corrupted image recovery [19], texture analysis [20], perceptual grouping [21], object matching and recognition [22], pattern mining [23]. All these studies facilitated retrieval procedures of the land surface parameters using the atmospheric correction techniques.

These procedures contributed to the pattern recognition of different objects on remote sensing images. As a result, hyperspectral remote sensing is widely used in different practical applications such as monitoring forest species [24]-[26], peat and forest fires identification [27], and many other environmental problems.

The Support Vector Machine (SVM) method is one of the most frequently used classifiers [28].

Initially, parallel hyperplanes are considered to separate a pair of classes, passing through the boundary points characterized by the feature distribution of these classes.

After that, the SVM method was extended to the non-linear case by using kernel transformation. The radial basis kernel is normally employed in practical applications to provide more exact classification and polynomial kernels are applicable in the cases when it is more important to provide the high computation speed.

The most general way to extend SVM to multiclass cases consists in applying the error correcting the output code model. Besides the usual "one-vs-all" and "one-vs-one" approaches, this method allows implementing the randomized approach which provides the optimal balance between calculation speed and classification accuracy.

The multiclass kernel SVM can be considered as one of the most perspective methods of hyperspectral image processing. In particular, this method was used in [25] for the classification of forest tree species using airborne hyperspectral imagery obtained from the CASI imaging spectrometer produced in Canada. The high spatial and spectral resolution of the images provided the possibility of effectively combining texture and spectral features that allowed in turn to achieve high accuracy of tree species recognition (appr. 86%). Such accuracy is comparable with the standard requirements of the ground based forest inventory.

The objective of this paper is to emphasize priorities of hyperspectral imagery processing procedures (hundreds of spectral channels) versus multispectral ones (up to ten spectral channels) in different applications such as agriculture and forestry, environmental protection and monitoring. First, some publications concerning the priority description in the outlined domain are reviewed.

Further, we describe our experience in airborne hyperspectral imagery processing and represent some results obtained for a selected test area. The ground-based measurements of the forest attributes are used to validate the mutual results of remote sensing forest inventory. Different classifiers are used to estimate their priorities and deficiencies in hyperspectral remote sensing imagery processing for the selected test area.

Instead of the common-used concept of vegetation indices (different combinations of the spectral bands of imaging spectrometers) [29]-[32], we used the optimization techniques of data processing to remove the possible redundancy due to the correlation between neighboring channels [33]. The optimization allows us to increase the stability of training of the classifiers used.

As a result, it is possible to gain information about the spatial distribution of pixels on the hyperspectral images and the texture of the forest areas with different species and ages [34].

Each measurement of spectral radiance or any derivative characteristics given by the imaging spectrometer can be interpreted as a point in the multidimensional space of features. These points might be clustering in the space giving useful information about the forest objects of different species and ages. As a result, the recognition procedures are realized using machine-learning algorithms of imagery processing. A conclusion is made that non-linear classifiers do have priorities compared to their linear analogs.

II. Comparative Analysis of Multispectral and Hyperspectral Techniques

In order to find the priorities of hyperspectral imagery processing compared to multispectral imagery, let us consider paper [35]. Here, estimates were obtained of the biomass for agricultural canopies using hyperspectral narrow-band indices calculated from the EO-1/Hyperion surface reflectance measurements, which were shown to have advantages compared to the broad-band multispectral indices of the high spatial resolution satellites (WorldView-2, IKONOS, GeoEye-1) as well as the lower spatial resolution satellites (MODIS and Landsat/ETM+). It is not clear which satellite system gives the better results in this indices approach tested for such important crops as alfalfa, cotton, rice and maize, but the ability of users to choose distinct values in this approach for improved crop biomass assessment surpasses the benefits coming with the higher spatial resolution of the other listed satellite sensors and the smoothed variability of crop biomass of the lower spatial resolution sensors.

The AVIRIS (Airborne Visible/Infrared Imaging Spectrometer) hyperspectral images were successfully employed in [36] for the assessment of fire severity and the environmental changes caused by fire. The results obtained revealed the priority of AVIRIS measurements in comparison with the broad-band spectral indices calculated using Landsat data. This was due to the fact that the separability of post-fire environments (char, green vegetation, non-synthetic vegetation and substrate) was higher in the hyperspectral case as compared to the multispectral one. Thus, the fractional cover estimates obtained from hyperspectral data resulted to be better than the benefits from multispectral data to assess fire severity.

One more example of priority of hyperspectral data compared to multispectral data is given in [37]. Here, both types of remote sensing data are used to assess the accuracy of salinity stress in sugarcane fields. The stress is caused by soil salinity in the sugarcane root zone collected at 191 locations in 25 testing fields. A Hyperion image compared to a Landsat ETM+ image along with field data was used for this purpose. The Hyperion data were shown to outperform Landsat data in the quantitative estimation of salinity stress and its mapping.

One more comparison of the post-fire consequences is analyzed in [38] using hyperspectral data from AVIRIS and multispectral data from Landsat. These consequences include ash, charred organic matter, soils and soil minerals, and dead, damaged, and living vegetation within the high spatial resolution (2.4 m pixel size) from AVIRIS data compared to Landsat ETM+ data. 10 classes of post-fire situations were analyzed within the selected area. The Landsat classification overestimated the cover by dry coniferous and ash classes and underestimated soil and green vegetation cover. It is not corresponding to real observations. As a result, the Burned Area Emergency Rehabilitation (BAER) map of burn severity areas did not capture the variable pattern of the post-fire surface by processing Landsat data, which are seen in the AVIRIS map in the detailed consideration.

Hyperspectral measurements can be also used for assessing the performance of perspective satellite instruments. This kind of work is presented in [39], where simulated medium resolution multispectral data of the polar orbiting satellite Sentinel-2 (European Space Agency) are compared to airborne hyperspectral data for tropical forests. The purpose of this comparison is understanding the ability of Sentinel-2 mission to classify forest types, areas with selected dominant species and tree groups of different functional guilds.

The advantage of using texture features in the considered classification problems is demonstrated. It is more important for multispectral Sentinel-2 data to have lower spectral and spatial resolution. The subtle nuances of the forest composition have to be taken into account in the classification techniques. These nuances are studied by using the classification results of the Support Vector Machine and Maximum Likelihood approaches.

To continue this part of studies in [40], the capabilities of existing and forthcoming satellite imagers (multispectral and hyperspectral) are compared to soil variables estimate (clay, sand, silt and organic carbon content). The hyperspectral imagers are shown to contribute to the improvement of the accuracy of soil variables estimation from bare soil imagery; however, this improvement is still too limited to allow an accurate quantitative estimation of soil texture and Soil Organic Carbon. The next generation of hyperspectral satellite imagers is designed to improve the situation.

The Vegetation Leaf Area Index (LAI) is the main parameter characterizing the relevant patterns by the narrow-band hyperspectral and traditional broad-band multispectral data [41]. This study uses the advantage of the LAI dataset collected at the same total time and the grain size by Landsat ETM+ and AVIRIS imagery in four different biomes. The sampled biome types included mixed hardwood-conifer and boreal conifer forests, row-crop agriculture and tall-grass prairie. It was shown that models based on the broad-band datasets predict the LAI values less accurately than those with selected subsets of AVIRIS channels. The Vegetation chlorophyll content can be obtained from narrow-band hyperspectral data as an alternative to broad-band multispectral data.

Corresponding estimates for the Mediterranean pine plantations in Spain are presented in [42]. The known leaf model PROSPECT-5 and radiative transfer model DART were employed for the retrieval purpose of modeling using available hyperspectral and multispectral satellite sensors in the form of ratios of measurements on the 750 and 710 nm wavelengths (the red-edge index) as well as on 800 and 560 nm. The high-resolution hyperspectral images allowed obtaining the strongest relationships in the chlorophyll content retrieval.

Hyperspectral narrow-band and multispectral broad-band indices were used in [43] to estimate evapotranspiration (ET) rates (mutual effect of soil moisture evaporation and vegetation transpiration). The ET rates give information about micro- and macro-scale climatic processes to monitor droughts, schedule irrigation, and assess crop water productivity over large areas. Ratio-based vegetation indices retrieved from optical remote sensing data are used for the estimates.

The study revealed that the hyperspectral narrow-band indices consistently explained a higher variability in ET than the indices obtained from the multispectral sensors. .

The problem of classification and mapping of tree species in tropical seasonal forests is considered in [44]. Airborne hyperspectral and simulated multispectral images of Brazilian Atlantic semi-deciduous forests in 450-2400 nm spectral range were used. Three different types of supervised classifiers were applied to recognize the species at the pixel level. The Linear Discriminant Analysis revealed better results compared to Kernel Support Vector Machines (linear and radial kernels) and Random Forests almost for all considered tests. The inclusion of shortwave infrared bands (SWIR, 1045–2400 nm) revealed the increase of accuracy from 70% up to 84% compared to using the visible/near-infrared (VNIR, 450–919 nm) bands.

The productivity retrieval of the leading world crops of cotton, wheat, maize, rice, and alfalfa is discussed in [45] for the NASA HyspIRI mission. That is the Hyperspectral Infrared Imager mission that is designed to study world ecosystems and provide information on natural disasters (droughts, wildfires, volcanoes etc) to retrieve types and conditions of vegetation covers. The main purpose of this publication consisted in modeling the crop productivity and discriminating crop types using available and perspective hyperspectral and multispectral imagers, though this mission is primarily designed to observe natural disasters. Overall, the crop biophysical models based on hyperspectral data and related narrow-band vegetation indexes explained approximately 25% wider variability compared to multispectral broad-band models.

To continue this short review concerning the comparative analysis of multispectral and hyperspectral techniques, we have to discuss our own experiments [46] in hyperspectral imagery processing using the domestic airborne hyperspectral instrument series produced in Russia and ground-based field campaign measurements on a test area. The estimation of accuracy of hyperspectral imagery processing was performed by using random resampling techniques such as cross-validation [47] and bootstrapping [48].

The Details of these methods are described in [49]-[52]. We elaborated an original approach to separate sunlit tops of trees, the completely shaded background of forest phyto-elements, and the partially illuminated and partially shaded features of the forest canopy on the images. The separation is conducted due to essentially different spectral features of these three categories of forest canopy. This is necessary because of the high spatial resolution of the imager (near 1 m) since random pixels on the images under processing are distributed in accordance with the three above categories that form the particular image, unless the boundaries between forest classes appears. The image producers ensure high values of signal-to-noise ratios of their device only for sunlit tops. Every forest class is represented by the alternation of the listed three categories of pixels for the forest canopy. The classification results were compared to separate plots on ground-based maps, which are needed to validate the information products of imagery processing. Thus, it is necessary to discriminate these forest canopy categories to recognize tree species and ages and estimate forest inventory parameters within the plots. That is why such complicated procedures are undertaken, which are not typical for Landsat data processing of lower spatial resolution.

III. Discussion

The analysis of publications [35]-[45] has shown that both spectral and texture features extraction from multispectral and hyperspectral images is an original process that cannot be solved in advance for every object in a particular scene. A necessity emerges to optimize the computational procedures of the objects pattern recognition having in mind the spectral and texture features for the scene depending on the spectral and spatial resolution of the type of imaging spectrometer.

Further, the results obtained by such airborne hyperspectrometer having both high spectral (287 spectral channels in visible and near infrared region) and spatial resolution (approximately 1 m at the flight altitude about 2 km) will be discussed.

The last version of the domestic hyperspectral instrument is given by Fig. 1 (the external view and its view in the delivery set). This imaging spectrometer is installed on a gyro-stabilized platform of the airborne carrier and may be installed on Unmanned Aerial Vehicles (UAV).

Appearance of AV-VD

Delivery set

Fig. 1. The domestic imaging spectrometer that is installed on an airborne gyro-stabilized platform for remote sensing

The instrumentation details are described in [46] operating in the spectral range 401-1017 nm together with the techniques of imagery processing elaborated by us. The algorithms for the retrieval of forest stand attributes are based on the optimization and classification methods listed below.

In the algorithms, the holdout cross-validation method [47], [48] was used to find regularized solution of the calculation problem that is too much sensitive to variations in the learning samples. This enables to select the information layers for a particular class of forest canopy pixels belonging to sunlit tops, half-shaded areas and completely shaded spaces between tree crowns on hyperspectral images. As a result, the separation of these information layers serves to improve the classification accuracy of forests species and ages.

In [49], the approach of supervised classification procedures for the land surface objects using their spectral and texture characteristics on hyperspectral images was improved. The improvement concerned the retrieval of biological productivity parameters for the recognized forest stand composition. Direct and inverse modelings were performed in terms of the projective cover and density of the forest canopy for the selected forest classes.

The Characteristic features of the information products obtained for the test area are presented. The results are compared to the ground-based forest inventory map and revealed the automation prospects of the recognition of forest ecosystems using hyperspectral images while employing the proposed apparatus and programming system of imagery processing.

Further, the results of machine-learning algorithms and optimization procedures concern the retrieval of productivity parameters for the related classes of forests [50]. The relevant procedures are based on solving the direct problem of atmospheric optics consisting in modeling the spectral characteristics of the forest canopy at different conditions and the inverse problem of forest parameters retrieval. The inverse modeling employs the relations between the projective and production characteristics to find parameters as the biomass of tree components and net primary production.

Paper [51] opens up details on the basic modeling approach concerning improvements of Bayesian classifier for airborne hyperspectral imagery processing.

The connectivity of pixels corresponding to different forest classes was described using the maximum a posterior probability and Markov random fields.

We introduced energy categories for the selected classes to estimate the measure between the spectral measurements and the theoretical functions approximating the processed images. Optimization procedures allowed to recognize forest classes taking into account thin differences in their spectral characteristics.

Thus, the correlated non-informative channels of imaging spectrometer are excluded from consideration.

To enhance the efficiency of processing hyperspectral images, in [52] the ability of different basic classifiers was considered. These are the metric classifier based Euclidean distance, the K nearest neighbors classifier with optimized incomplete enumeration, the parametric Bayesian classifier based on Gaussian Mixture Model, and the kernel Support Vector Machine extended to multiclass classification by using the error correcting output codes. It was shown [52] that nonlinear classifiers have significant advantages for the considered problem of classification of the vegetation cover.

To further discuss the listed classification methods of hyperspectral imagery processing, let us consider the comparison of their application with ground-based forest inventory procedures. Figs. 2-4 give some results of such comparison.

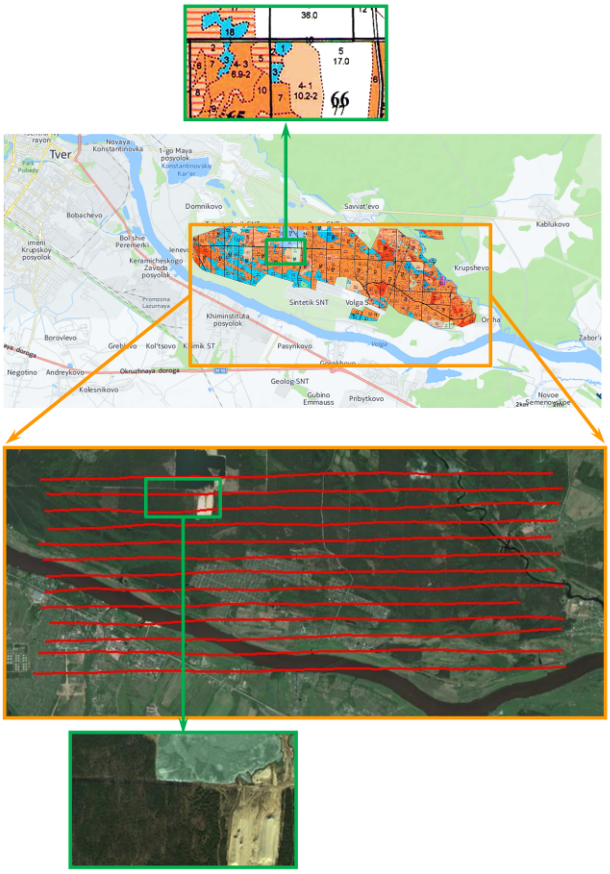

Fig. 2. Area within Savvatyevskoe forestry Tver region (Russia) covered by airborne hyperspectral measurements and the test region. The map of the test area includes two frames: of the orange color with the ground-based forest inventory color representation of the quarters and plots inside them; of the green color inside the area with its internal forest inventory map (the upper frame) and the RGB-synthesized image (the lower frame). Locations of the airborne tracks are indicated by the red lines on the lower picture

Fig. 2 depicts the area of size 10×4 km (highlighted by the orange frame), where the airborne hyperspectral measurements were performed. The particular sub-area (highlighted by green frame) was used for the quantitative comparison of processing results and ground-based forest inventory data. The RGB-synthesized image of this test area serves for the visual analysis of objects on the considered scene.

The entire test area was encompassed by 13 overlapped images obtained from the airplane equipped on the same gyro-stabilized platform by the imaging spectrometer and photo-camera. The location of the direct and opposed flight tracks are represented by red color lines in the lower part of the scene (Fig. 2).

The Parameters of sets containing spectral radiances of forest classes (forest areas of different species and age) are given by Table I. These sets were used for training the classification algorithm used.

Pine species of the age from the young forest (13 years old) to the mature forest (136 years old) with near to ten years resolution are prevailing.

TABLE I
PARAMETERS OF THE SPECTRAL RADIANCE ENSEMBLES FOR THE SELECTED FORESTED AREA

Species	Age	Number of spectra	Local time of the airplane tracks
Pine	13	1046	11-10-57
	16	2428	11-31-32
	26	2061	12-05-23
	36	447	11-10-57
	47	5025	11-17-58
	56	1807	11-46-25
	66	7551	11-52-48
	76	1557	11-52-48
	76	4019	11-59-25
	86	2055	11-46-25
	96	3156	11-38-02
	106	2191	11-59-25
	116	644	11-24-25
	126	1932	11-04-17
	136	695	11-46-25
Birch	16	1729	11-31-32
	51	1634	11-38-02
	71	5656	11-46-25
Aspen	11	2545	11-38-02
Elm	–	534	10-47-53

Each hyperspectral image corresponding to red lines on the lower image of Fig. 2 has 500 pixels across the flight direction and 10000-14000 pixels along the flight direction. The flight altitude is approximately 2 km above the ground level with typical deviations of about 10 m. The maximum deviation is 58 m. Thus, the spatial resolution across the track is stable and amounts to 1.1 m. The pixel size along the track depends on the flight speed and changes within 0.66-0.91 m.

The landscape of the test area contains different types of natural and artificial objects: water bodies, open soils, roads, buildings, forests, grasslands. As we can see from Fig. 2, about half of the area is covered by forests, therefore the ground-based forest inventory maps are available. A field campaign was performed to obtain geo-botanical descriptions and to more precisely define forest typology and other parameters indicated in the available forest inventory for the test area. These works allowed to improve validation and ground truth estimates.

The typical forest inventory procedure in Russia usually deals with obtaining ground-based maps for a particular area as separated compartments and plots within them. The maps are represented by specific colors (the plots for prevailing birch species by blue; the same for prevailing pine species by orange; forest plantations are denoted by the horizontal hatching, etc.). The darker color characterizes more aged forests for the listed species.

Each compartment and plot has its own number on these maps. For each plot on the map are usually given the following data: an identity number, the average age of the dominant tree species, a total area of the plot expressed in square meters and the cite index characterizing wood quality. The higher values of cite index correspond to the sluggish growth and to the low quality of stem wood. Not all plots are represented by this full set of numbers on Fig. 2. The full list of ground-based forest inventory includes the following parameters: the type of plant growth (natural or artificial), the number of quarters and plots, square meters of their areas, their wood volumes and ages, the wood quality, the density of each plant, the forest typology concerning inter-crown vegetation, the average diameter and height of each stand, species composition of the plots. These are typical vector layers for the forest recognition while using the related cartographic materials.

Two frames of Fig. 2 (of the orange and green color) represent the entire test area and its internal part, respectively. This particular part of the terrain includes the sand pit filled in with water (visible on the upper right corner), bare soils (at the lower right corner) and large amounts of forest vegetation with the pine and birch trees prevailing at the remaining part of the green color frame. In particular, the sand pit in the lower right corner consists in two sand hills divided by the road and scare vegetation denoted by number 66 at the upper frame. At the lower frame of the RGB-synthesized image this area looks as a completely forested one. Our intention is to recognize these forests of different species and age along with the other objects available on this scene using our original algorithmic and programmatic tool of hyperspectral imagery processing.

The recognition results of the objects within the green frame by the Bayesian classifier with the Gaussian mixture model of radiances are represented in Figs. 3. In general, these objects are given by the water body in the upper right corner (blue color on Fig. 3(a)), bare soils with scare vegetation in the lower right corner (yellow and magenta colors) and by the forests of different species and age in the remaining part of this scene (prevailing green color). The magenta color corresponds to the unrecognized objects, which are mainly located on the coast of the sand pit, on the road and between different slopes of the pit. These pixels mean that the corresponding spectral portraits are likely to be absent in the training set. That is why the related objects are referred to as unrecognized. The aspen pixels are apparent for plots 1, 2, 7 and 16.

The spatial distribution of the main types of forest objects within the relevant plots represented by white digits from 1 to 18 can be seen in Fig. 3(a). The boundaries of these plots are depicted by white lines, ground-based forest inventory data can be seen from Table II for each plot. Number of stands within each plot together with the average age, the greenness class (from 1 to 3), the average diameter of the stands, their height and species composition are given in Table II. In particular, we can see young forest at plot 16, the lowest greenness class at plot 18 and the species composition from the pure pine plots (10P, numbers 1, 4, 7, 9, 14, 17) to the half pine and birch areas (5P5B, plot 8).

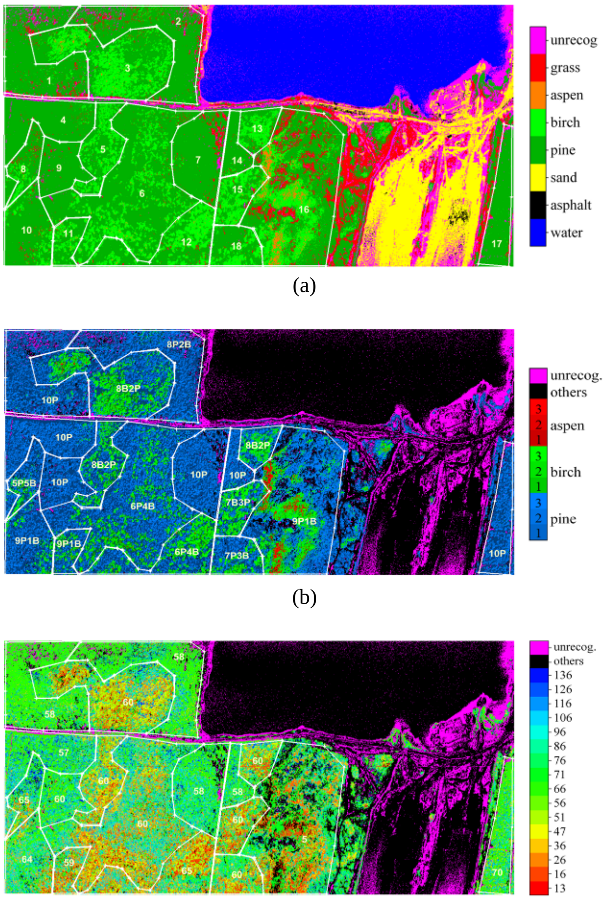

Figs. 3. Classification results using parametric Bayesian classifier based on Gaussian mixture distribution: (a) – main types of the objects on this terrain; (b) – forest species (taking into account gradations of the forest canopy illumination by the Sun); (c) – the average forest ages within each plot (years)

TABLE II
FOREST INVENTORY DATA FOR THE TEST AREA

Plot numbers	Stand volume m3/ha	Age, years	Site index	Diameter cm	Heightm	Species compo-sition
1	260	58	2	18	18	10P
2	210	58	2	18	17	8P2B
3	180	60	2	18	20	8B2P
4	220	57	2	16	16	10P
5	180	60	2	18	20	8B2
6	280	60	2	18	19	6P4B
7	210	58	2	18	17	10P
8	300	65	2	20	20	5P5B
9	200	60	3	16	16	10P
10	260	64	2	18	18	9P1B
11	210	59	2	18	17	9P1B
12	300	65	2	20	20	6P4B
13	250	60	2	20	23	8B2P
14	220	58	3	16	16	10P
15	260	60	2	20	23	7B3P
16	30	5	2	2	3	9P1B
17	220	70	2	20	20	10P
18	300	60	1	20	20	7P3B

The retrieval of the age composition in the considered forest plots is represented in Fig. 3(c).

The results obtained depend on the dominant species of the plot (the pine or birch in this case). As we can see, the remote sensing estimates of the age composition do not agree with the ground forest inventory so well as it was for the species composition.

In particular, plots 1, 2, 4 and 7 contain trees with the same age and site index (see Table II). The age composition of plots 1 and 2 is reproduced well enough; however, the significant part of stands within plots 4 and 7 is classified as mature forest (age is 90 years and older) which does not agree with ground based data. This non-conspiracy can be partly explained by the different origins of the stands: plots 1 and 2 contain forest plantations and plots 4 and 7 have a natural origin.

The age of stands within plot 14 is overestimated in 15-20 years. However, the pixels of plot 17 are classified as pine trees of 70-80 years old, which is in agreement with the ground-based forest inventory data.

The former logging places are seen for plot 16, where there seems to be re-growth vegetation with young forests nominated as 9P1B. A certain amount of pixels containing aspen trees can also be seen, in accordance with the results obtained.

Root mean square errors of retrieval of the forest species composition (in percent) are represented by the colored bars for three considered gradations of canopy illumination (Fig. 4). The natural level of errors due to the boundary pixels of the plots is represented by the black bar. The 10% error corresponds to the requirements of the ground-based forest inventory.

We should also note that the age retrieval of the birch stands is usually underestimated compared to the inventory data. 28% of pixels corresponding to birch stands are classified as 16 years old, 49% as 51 years old and the remaining 23% as 71 years old. Thus, the pixels corresponding to the mixed forest areas are classified as being younger than the pixels within pure pine areas. The pine prevailing plots, on the contrary, are normally classified as being older than it is represented in ground data. The worst situation is for young forests. In particular, plot 16 should contain young pine forest following the inventory information. However, the pixels classified as the young forest mainly correspond to the birch stands. The pine stands in the right bottom corner of this plot are classified as the ripening forest.

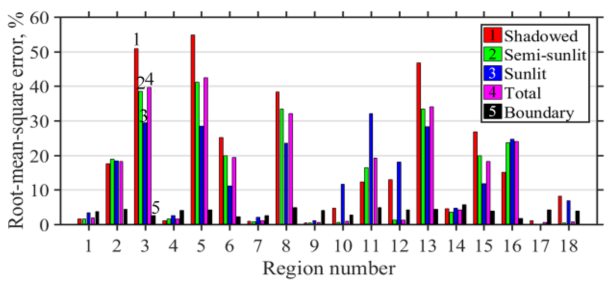

Fig. 4. The classification errors for the proposed model of the pattern recognition

Thus, it is possible to separate the contribution of the considered gradations of illumination of tree crowns for the selected regions.

The errors are higher for the plots with prevailing birch stands. Also, we can see the pixels within the plot 16 classified as aspen, which is not available in accordance with forest inventory data.

The total weighted error amounts to 8.3%, for the shadowed pixels it is 9.7%, for the partly illuminated – 8.2% and for the completely illuminated – 7.7%. These errors occur to be not larger than those obtained in the ground-based forest inventory procedures.

The pixels classified as the aspen amount to 0.6% of the total number of the forest pixels.

The relatively low errors of the pattern recognition of forests as compared to the similar errors of the ground-based forest inventory can serve to replace these laborious works by the proposed hyperspectral imagery processing.

IV. Conclusion

The short analysis of publications dealing with imagery processing has shown that both spectral and texture features extraction from multispectral and hyperspectral images are original processes that cannot be solved in advance for any object on a particular scene.

A necessity emerges to optimize the computational procedures of the objects pattern recognition having in mind the spectral and texture features of the scene depending on the spectral and spatial resolution of the type of imaging spectrometer used.

Therefore, some results obtained by such airborne hyperspectrometer having both high spectral resolution (near to 200 spectral channels in visible and near infrared region) and high spatial resolution (near to 1 m from the altitudes 1.5-2 km) were discussed.

The analysis enabled to compare the results of the imaging spectrometer data processing for forest canopies of different species and ages with the common-used ground-based forest inventory procedures. The results have shown that the accuracy of forest attributes retrieval is not worse than this routine laborious work of forest inventory.

That contributes to the prospects of forest inventory in the newly defined domain of hyperspectral imagery processing.

To enhance the computational efficiency it is required to create parallel algorithms of hyperspectral imagery processing. The first attempts in this direction are described in [53]. However, the results of data parallel processing require a separate study.

Acknowledgements

These results are obtained under funding support from the Russian Science Foundation (No. 16-11-00007), and the Russian Fund for Basic Research (No. 16-01-00107).

References

[1] T. R. Loveland, J. L. Dwyer, Landsat: Building a strong future, *Remote Sens. Environ.* 122 (2012), 22-29.

[2] B. L. Markham, D. L. Helder, Forty-year calibrated record of earth-reflected radiance from Landsat: A review, *Remote Sens. Environ.* 122 (2012), 30-40.

[3] M. C. Hansen, T. R. Loveland, A review of large area monitoring of land cover change using Landsat data, *Remote Sens. Environ.*122 (2012), 66-74.

[4] D. Rogers, T. Tanimoto, A computer program for classifying plants, *Science* 132 (1960), 1115-1118.

[5] R. E. Osteen, J. T. Tou, A clique detection algorithm based on neighborhoods in graphs, *Int. J. Computer Info. Sci*. 2, 4 (1973), 257-268.

[6] V. V. Kozoderov, E. V. Dmitriev, V. P. Kamentsev, Cognitive technologies for processing optical images of high spatial and spectral resolution, *Atmospheric and Oceanic Optics* 27, 6 (2014), 556-563.

[7] M. F. Tompsett, G. F. Amelio, W. J., Jr. Bertram, R. R. Buckley, W. J. McNamara, J. C., Jr. Mikkelsen, D. A. Sealer, Charge-coupled imaging devices: Experimental results, *IEEE Transactions on Electron Devices* 18, 11 (1971), 992-996.

[8] A. F. H. Goetz, G. Vane, J. E. Solomon, B. N. Rock, Imaging spectrometry for Earth remote sensing, *Science* 228 (1985), 1147-1153.

[9] V. V. Kozoderov, T. V. Kondranin, E. V. Dmitriev, V. P. Kamentsev, A system for processing hyperspectral imagery: application to detecting forest species, *Int. J. Remote Sens.* 35, 15 (2014), 5926-5945.

[10] E. Binaghi, I. Gallo, M. Pepe, A cognitive pyramid for contextual classification of remote sensing images, *IEEE Transactions Geosci. Remote Sens. 41,* 12 (2003), 2906-2922.

[11] V. V. Kozoderov, E. V. Dmitriev, V. P. Kamentsev, System for processing of airborne images of forest ecosystems using high spectral and spatial resolution data, *Izvestiya, Atmospheric and Oceanic Physics* 50, 9 (2014), 943-952.

[12] P. J. Sellers, F. G. Hall, G.Asrar, D. E. Strebel, R. E. Murthy, An Overview of the First International Satellite Land Surface Climatology Project (ISLSCP) Field Experiment (FIFE), *J. Geoph. Res. 97,* D17 (1992), 18345-18371.

[13] R. O. Duda, P. E. Hart, *Pattern Classification and Scene Analysis* (J. Wiley, 1973).

[14] J. T. Tou, R. C. Gonzalez, *Pattern Recognition Principles* (Addison-Wesley, 1974).

[15] S. Z. Li, *Markov Random Field Modeling in Computer Vision* (Springer-Verlag, 1995).

[16] V. V. Kozoderov, Assessment of Effect of the Atmosphere as a Clutter in Recognition of Natural Formations from Space, *Airspace Studies of the Earth. Remote Sensing Data Processing Using Computer Means*, (Moscow, Nauka, 1978, pp. 24-35).

[17] P. J. Curran, G. M. Foody, K. Ya. Kondratyev, V. V. Kozoderov, P. P. Fedchenko, *Remote sensing of soils and vegetation in the USSR* (Taylor & Francis, 1990).

[18] K. Ya. Kondratyev, V. V. Kozoderov, O. I. Smokty, *Remote Sensing of the Earth from Space: Atmospheric Correction* (Springer-Verlag, 1992).

[19] Y. P. Hung, D. B. Cooper, B. Cernuschi-Frias, Asymptotic Bayesian surface estimation using an image sequence, *Int. J. Comput. Vis.* 6, 2 (1991), 105-132.

[20] A. K. Jain, R. P. W. Duin, J. Mao, Statistical pattern recognition: a review, *IEEE Trans. Pattern Anal. Mach. Intell.* 22, 1 (2000), 4-37.

[21] L. Herault, R. Horaud, Figure-ground discrimination: A combinatorial optimization approach, *IEEE Trans. Pattern Anal. Mach. Intell.* 15, 9 (1993), 899-914.

[22] N. S. Friedland, A. Rosenfeld, Compact object recognition using energy-function based optimization, *IEEE Trans. Pattern Anal. Mach. Intell.* 14, 7 (1992), 770-777.

[23] J. Han, H. Cheng, D. Xin, X. Yan, Frequent pattern mining: current status and future directions, *WIREs Data Min. Knowl. Discov.* 15, 1 (2007), 55-86.

[24] M. Dalponte, L. Bruzzone, L. Vescovo, D. Gianelle, The role of spectral resolution and classifier complexity in the analysis of

hyperspectral images of forest areas, *Remote Sens. Environ.* 113, 11 (2009), 2345-2355.
[25] Y. Dian, Z. Y. Lib, Y. Pang, Forest Tree species Classification Based on Airborne Hyperspectral Imagery, *Proc. of SPIE 8921 (2013)*, 892107-(1-7).
[26] J. Lee et al, Individual Tree Species Classification From Airborne Multisensor Imagery Using Robust PCA, *IEEE Journal of Selected topics in applied earth observations and remote sensing* 9, 6 (2016), 2554-2567.
[27] V. V. Kozoderov, T. V. Kondranin, E. V. Dmitriev, V. P. Kamentsev, Mapping forest and peat fires using hyperspectral airborne remote-sensing data, *Izv., Atmos. Ocean. Phys*. 48, 9 (2012), 941-948.
[28] N. Cristianini, J. Shawe-Taylor, *An Introduction to Support Vector Machines and Other Kernel-based Learning Methods*, first ed. (Cambridge: Cambridge University Press, 2000).
[29] T. P. Higginbottom, E. Symeonakis, Assessing Land Degradation and Desertification Using Vegetation Index Data: Current Frameworks and Future Directions, *Remote Sens*. 6 (2014), 9552-9575.
[30] A. Viña, A. A. Gitelson, A. L. Nguy-Robertson, Y. Peng, Comparison of different vegetation indices for the remote assessment of green leaf area index of crops, *Remote Sens. Environ.* 115 (2011), 3468-3478.
[31] S. S. Panda, D. P. Ames, Application of Vegetation Indices for Agricultural Crop Yield Prediction Using Neural Network Techniques, *Remote Sens.* 2 (2010), 673-696.
[32] F. V. Eroshenko , S. A. Bartalev, I. G. Storchak, D. E. Plotnikov, The possibility of winter wheat yield estimation based on vegetation index of photosynthetic potential derived from remote sensing data, *Sovremennye problemy distantsionnogo zondirovaniya Zemli iz kosmosa,* 13, 4 (2016), 99-112.
[33] V. V. Kozoderov, E. V. Dmitriev, Remote sensing of soils and vegetation: pattern recognition and forest stand structure assessment, *Int. J. Remote Sens.* 32, 3 (2011), 5699-5717.
[34] E. V. Dmitriev, V. V. Kozoderov, Optimization of spectral bands for hyperspectral remote sensing of forest vegetation, *Proc. SPIE, Remote Sensing for Agriculture, Ecosystems, and Hydrology,* 8887 (2013), 1-10.
[35] M. Marshall, P. Thenkabail, Advantage of hyperspectral EO-1 Hyperion over multispectral IKONOS, GeoEye-1, WorldView-2, Landsat ETM+, and MODIS vegetation indices in crop biomass estimation, *ISPRS J. of Photogrammetry and Remote Sens*. 108 (2015), 205-218.
[36] S. Veraverbeke, E. N. Stavros, S. J. Hook, Assessing fire severity using imaging spectroscopy data from the Airborne Visible/Infrared Imaging Spectrometer (AVIRIS) and comparison with multispectral capabilities, *Remote Sens. Environ.* 154 (2014), 153-163.
[37] S. Hamzeh, A. A. Naserib, S. K. AlaviPanaha, H. Bartholomeusc, M. Herold, Assessing the accuracy of hyperspectral and multispectral satellite imagery for categorical and quantitative mapping of salinity stress in sugarcane fields, *Int. J. of Applied Earth Observation and Geoinformation* 52 (2016), 412-421.
[38] R. F. Kokaly, B. W. Rockwell, S. L. Haire, T. V. V. King, Characterization of post-fire surface cover, soils, and burn severity at the Cerro Grande Fire, New Mexico, using hyperspectral and multispectral remote sensing, *Remote Sens. Environ.* 106 (2007), 305-325.
[39] G. V. Laurin, N. Puletti, W. Hawthorne, V. Liesenberg, P. Corona, D. Papale, Q. Chen, R. Valentini, Discrimination of tropical forest types, dominant species, and mapping of functional guilds by hyperspectral and simulated multispectral Sentinel-2 data, *Remote Sens. Environ*. 176 (2016), 163-176.
[40] F. Castaldi, A. Palombo, F. Santini, S. Pascucci, S. Pignatti, R. Casa, Evaluation of the potential of the current and forthcoming multispectral and hyperspectral imagers to estimate soil texture and organic carbon, *Remote Sens. Environ*. 179 (2016), 54-65.
[41] K. S. Lee, W. B. Cohen, R. E. Kennedy, T. K. Maiersperger, S. T. Gower, Hyperspectral versus multispectral data for estimating leaf area index in four different biomes, *Remote Sens. Environ.* 91 (2004), 508-520.
[42] R. MaNavarro-Cerrillo, J. Trujillo, M.Sánchez de la Orden, R. Hernández-Clemente, Hyperspectral and multispectral satellite sensors for mapping chlorophyll content in a Mediterranean Pinus sylvestris L. plantation, *Int. J. of Applied Earth Observ. and Geoinform.* 26 (2014), 88-96.
[43] M. Marshall, P. Thenkabail, T. Biggs, K. Post, Hyperspectral narrowband and multispectral broadband indices for remote sensing of crop evapotranspiration and its components (transpiration and soil evaporation), *Agricultural and Forest Meteorology* 218-219 (2016), 122-134.
[44] M. P. Ferreira, M. Zortea, D. C. Zanotta, Y. E. Shimabukuro, de Souza F. C. R., Mapping tree species in tropical seasonal semi-deciduous forests with hyperspectral and multispectral data, *Remote Sens. Environ.* 179 (2016), 66-78.
[45] I. Mariotto, P. S. Thenkabail, A. Huete, E. T. Slonecker, A. Platonov, Hyperspectral versus multispectral crop-productivity modeling and type discrimination for the HyspIRI mission, *Remote Sens. Environ.* 139 (2013), 291-305.
[46] V. V. Kozoderov, T. V. Kondranin, E. V. Dmitriev, A. A. Sokolov, Retrieval of forest stand attributes using optical airborne remote sensing data, *Optics Express* 22, 13 (2014), 15410-15423.
[47] R. Kohavi, A study of cross-validation and bootstrap for accuracy estimation and model selection, *Int. Joint Conf. on Artificial Intell. (IJCAI) (1995)* 528-535.
[48] T. Hastie, R. Tibshirani, J. Friedman, *The Elements of Statistical Learning; Data Mining, Inference, and Prediction*, second ed. (Springer, 2008).
[49] V. V. Kozoderov, T. V. Kondranin, E. V. Dmitriev, V. P. Kamentsev, A system for processing hyperspectral imagery: application to detecting forest species, *Int. J. Remote Sens.* 35, 15 (2014), 5926-5945.
[50] V. V. Kozoderov, E. V. Dmitriev, A. A. Sokolov, Improved technique for retrieval of forest parameters from hyperspectral remote sensing data, *Optics Express* 23, 24 (2015), A1342-A1353.
[51] V. V. Kozoderov, T. V. Kondranin, E. V. Dmitriev, V. P. Kamentsev, Bayesian classifier applications of airborne hyperspectral imagery processing for forested areas, *Adv. Space Res.* 55, 11 (2015), 2657-2667.
[52] V. V. Kozoderov, E. V. Dmitriev, Testing different classification methods in airborne hyperspectral imagery processing, *Optics Express* 24, 10 (2016), A956-A965.
[53] A. Plaza, J. A. Benediktsson, J. W. Boardman, J. Brazile, L. Bruzzone, G. Camps-Valls, J. Chanussot, M. Fauvel, P. Gamba, A. Gualtieri, M. Marconcini, J. C. Tilton, G. Trianni, Recent advances in techniques for hyperspectral image processing, *Remote Sens. Environ.* 113 (2009), 110-122.

Authors' information

[1]M.V. Lomonosov Moscow State University, Leninskiye Gory, GSP-1, Moscow, 119991, Russia.
E-mail: vkozod@mail.ru

[2]Moscow Institute of Physics and Technology (State University), Institutskiy per., 9, Dolgoprudny, Moscow Region, 141700, Russia.
E-mail: kondr@kondr.rector.mipt.ru

[3]Institute of Numerical Mathematics of Russian Academy of Science, ul. Gubkina, 8, Moscow, Moscow, 119333, Russia.
E-mail: yegor@mail.ru

Vladimir V. Kozoderov, Prof., Dr. of Physical and Mathematical Sci., Head of remote sensing Earth sciences sector in Earth Science Museum of M.V. Lomonosov Moscow State University, Laureate of the Governmental Prize of Russian Federation in the field of science and technology for the work "Elaboration of methods and technologies of remote sensing aerospace monitoring of natural media" (2002). He is the author and co-author of more than 400 works in leading domestic and foreign publication series, including 15 monographs. His main scientific interests are: methods, algorithms and software tools of remote sensing data processing and comparisons with ground-based discrete measurements.

He was the scientific leader (late 1980-s – beginning 1990-s), from Russian side, in the First ISLSCP Experiment, where ISLSCP is International Satellite Land Surface Climatology Project with joint participation of scientists and engineers from USA, Russia, Canada, United Kingdom and France. Now he deals with automation of natural and anthropogenic objects pattern recognition on aerospace multispectral and hyperspectral images using different classifiers (computational procedures) with the objects spectral and texture feature selection.

Timofei V. Kondranin Doctor of Sciences (Physics & Maths), Professor. Head of the "Systems, Devices and Methods of GeoSpace Physics" Department of the Moscow Institute of Physics and Technology (State University). Laureate of the Prize of the President of the Russian Federation in the field of education for the work "New direction in the system of training highly qualified specialists in the field of Space science and technology on the basis of integration of fundamental and applied education using modern information technologies" (2003). Research interests: research, development and application of aerospace optic-electronic remote sensing instruments. Doctor Kondranin T.V. took part in the development and flight tests of visible and near infrared range hyperspectral camera as part of the additional on-board equipment of the experimental research Small Spacecraft for Fundamental Space Research (SSC-FSR) PN1, which worked in orbit from July 22, 2012 to June 20, 2013. He published more than 170 works in leading Russian and foreign journals.

Egor V. Dmitriev PhD (Physics & Maths), senior staff scientist of the Institute of Numerical Mathematics of the Russian Academy of Science. Education: Moscow Institute of Physics and Technology (State University) – MPhil, Institute of Numerical Mathematics of the Russian Academy of Science – PhD. He is the author and co-author of 32 articles in Russian and international journals on remote sensing problems and of 2 monographs.